



# Design and Monte Carlo Simulation of a Novel Irradiation Device

Xiaoxiao Li, Yi Gu, Baolin Song

College of Nuclear Technology and Automation Engineering, Chengdu University of Technology, Chengdu, China

Email: LiXiaoxiao95@qq.com

**How to cite this paper:** Li, X.X., Gu, Y. and Song, B.L. (2023) Design and Monte Carlo Simulation of a Novel Irradiation Device. *Open Access Library Journal*, 10: e10886.

<https://doi.org/10.4236/oalib.1110886>

**Received:** October 15, 2023

**Accepted:** November 12, 2023

**Published:** November 15, 2023

Copyright © 2023 by author(s) and Open Access Library Inc.

This work is licensed under the Creative Commons Attribution International License (CC BY 4.0).

<http://creativecommons.org/licenses/by/4.0/>



Open Access

## Abstract

In order to facilitate the calibration and scale of pyroelectric detectors for environmental dose monitoring, a new simple standard irradiation device was designed. Through Monte Carlo software, the uniformity of radiation field, absorbed dose of pyroelectric detector and scattering contribution rate of this device are simulated. The simulation results show that the new simple standard irradiator satisfies the national standards and can fulfill the calibration and scaling requirements of pyroelectric detectors for environmental dose monitoring.

## Subject Areas

Nuclear Physics

## Keywords

Thermoluminescence Detector, Ionizing Radiation, Irradiance Device, Dose Monitoring

## 1. Introduction

In the field of personal and environmental dose monitoring, dose monitoring is mainly carried out using thermoluminescence detectors (TLD), which are more convincing in the evaluation of environmental radiation levels because of their cumulative dose function, which allows them to be placed for a long period of time in the radiation field of interest and to record the radiation dose for the entire monitoring time period [1]. TLD rely on pyrophosphors to record the dose of ionizing radiation received. Different pyrophosphor detectors contain different amounts of pyrophosphors, which can lead to different radiation responses, so the use of TLD requires a standard irradiator to calibrate and scale them [2] [3]. However, standard irradiators are complicated and expensive to build, and

only a few research institutes have them. In order to facilitate the calibration and scaling of TLD, a simple irradiator suitable for commonly used standard work sources was designed. The device is designed to produce a reference dose rate of 10 uGy/h, *i.e.*, only 1/100 of the normal monitoring time is needed to reach the cumulative dose of the TLD, and through the design of the environmental background shielding, scattering cavity, and the collimator, it is ensured that the radiation field performance indexes can meet the standard specification requirements.

## 2. Irradiator Design

Combined with the use of demand and relevant standards, the irradiator needs to be able to irradiate a large number of TLD at one time, and to meet the requirements of the standard specifications in terms of safety, uniformity, scattering contribution rate and other indicators. The designed irradiator mainly consists of radiation source, scattering chamber, collimator, shielding chamber, pyroluminescent pallet, low-speed motor and arc attenuator. Among them, the shielding chamber is a cylinder with a height of 620 mm, an inner diameter of 258 mm, a thickness of 100 mm, and a material of Pb; the scattering chamber has an inner diameter of 58 mm, a depth of 50 mm, an outer diameter of 118 mm, a height of 80 mm, and a material of Cu; the collimator reference GB/T 12162. 1-2000 recommended collimator design, using seven layers of 8 mm after the tungsten alloy grating (W89%, Ni7%, Cu4%) composed of density of 17 g/cm<sup>3</sup> [4], the spacing of 12 mm, the radius of 50 mm, the lowest layer of the radius of the incidence aperture of 1mm, the opening angle of 12°; the radioactive source is an aged <sup>137</sup>Cs standard source with an activity of 2 × 10<sup>8</sup> Bq.

The structure of the irradiation device is shown in **Figure 1**, wherein 1 is a shielding chamber; 2 is a thermoluminescent pallet; 3 is a thermoluminescent pallet support; 4 is an arc attenuator; 5 is a collimator; 6 is a radioactive source; 7 is a radioactive source support block; 8 is a scattering cavity; and 9 is a slow motor.

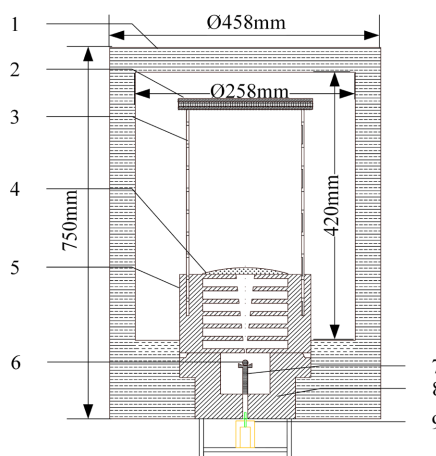


**Figure 1.** Irradiator design drawing.

## 2.1. Shield Design

According to GB/T 17568-2019 [5], under the premise of designing the maximum amount of loaded sources, the average dose rate generated by radiation from a radioactive source should be no more than 2.5  $\mu\text{sv/h}$  at a distance of 30 cm from the surface of the shielding body. In the design the material of the scattering chamber is copper and the main material of the lead chamber is lead. The scattering chamber is installed inside the lead chamber, as shown in **Figure 2**, and the radiation shielding is mainly borne by the lead chamber. The following is the shielding thickness design:

$$K_a^0 = A\Gamma_k / R^2 . \quad (1)$$

$$K_a^1 = A\Gamma_k e^{-\mu x} / R^2 . \quad (2)$$

Equation (1) is the dose rate calculation for the reference point without shielding and Equation (2) is the dose rate calculation for the reference point with shielding [6].

In the equation,  $A$  is the activity of the radioactive source with the value of  $2 \times 10^8$  Bq,  $\Gamma_k$  is the air specific kinetic energy constant of  $^{137}\text{Cs}$  with the value of  $0.079 \mu\text{Gy}\cdot\text{h}^{-1}\cdot\text{m}^2\cdot\text{MBq}^{-1}$ ,  $R$  is the measurement distance with the value of 0.3 m,  $\mu$  is the linear attenuation coefficient of the shielding material,  $x$  is the thickness of the shielding material,  $K_a^0$  is the air specific kinetic energy rate without shielding, and  $K_a^1$  is the air specific kinetic energy rate after the shielding. The specific kinetic energy rate of air at 30 cm is  $175.6 \mu\text{Gy/h}$  by Equation (1), and the minimum shielding thickness is 3.3 cm according to the maximum reference dose value of  $2.5 \mu\text{Gy/h}$  after shielding. The design thickness of the lead chamber is 10 cm, which meets the relevant requirements.

## 2.2. Charged Particle Equilibrium

The TLD shall meet the charged particle equilibrium when in calibration. The thermoluminescent pallet material is plexiglass, which is mainly used for placing the TLD in calibration and provides the condition of charged particle equilibrium. According to the beta particle range equation

$$R = 0.412E^{(1.265-0.0954\ln E)} . \quad (0.01 \text{ MeV} < E < 2.5 \text{ MeV}) \quad (3)$$

where  $R$  is the mass range of electrons in low  $z$  matter ( $\text{g}\cdot\text{cm}^{-2}$ ) [6], at the same time the density of plexiglass is  $1.19 \text{ g/cm}^3$ , then the range is  $d = R/\rho = 0.202156$  cm. the design of thermoluminescent pallets on the upper and lower layers of the thickness of 3 mm, to be able to satisfy the balance of charged particles, the structure is shown in **Figure 2**.

## 2.3. Radiation Field Uniformity Study

According to the requirements of JJG 593-2016 [7], at the calibration point, the homogeneous area of the radiation beam should be able to completely cover the examined dosimeter, and the inhomogeneity of this area should be no more than 5%.

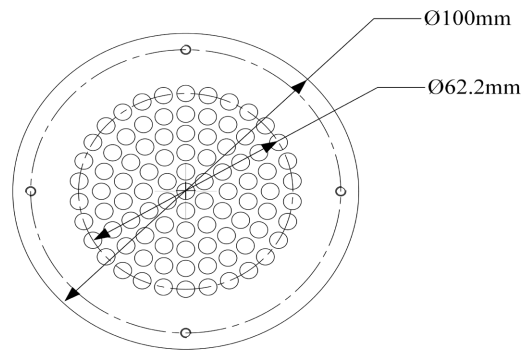


**Figure 2.** Thermoluminescent pallet design drawing.

The radius of the irradiation field is divided into ten equal parts, and the specific kinetic energy rate of air release at each point is calculated according to Equation (1), and the homogeneity of the reference radiation field is finally obtained. The results are shown in **Table 1**, and the inhomogeneity of the irradiation field is 1.09%, which meets the relevant requirements.

#### 2.4. Arc Attenuator Study

The role of the arc attenuator is used to improve the uniformity of the reference radiation field, as well as to reduce the low-energy scattering of the reference ray beam, taking into account the functional requirements of the arc attenuator and the material requirements, graphite is the main material of the arc attenuator. Meanwhile, considering the processing difficulty of the arc graphite and the new scattered rays brought by the over-thick graphite, an attenuator with the edge of the arc attenuator 1mm thick is used. According to the Equation (2) the radiation field dose value is corrected to the same (the dose value of the edge 1 mm), the thickness of each correction point of the arc attenuator is shown in **Table 2**, and the theoretical design is shown in **Figure 3**.

Based on the required attenuator thickness at each reference point, the attenuator is fitted to a hemisphere with a radius of 90.76 mm using matlab to obtain the curved attenuator.

### 3. Monte Carlo Simulation

According to the requirements of GB/T 12162.1-2000, the contribution of scattered radiation from the reference radiation field should not exceed 5% of the total air-specific kinetic energy rate, and the variation of the air-specific kinetic energy rate should not exceed 5% over the entire sensitive volume of the detector at each test point. As well as in accordance with the requirements of JJG 593-2016, the homogeneous area of the radiation beam at the calibration point should be able to completely cover the examined dosimeter, and the inhomogeneity of this area should not exceed 5%.

The following simulations will be carried out in terms of the air specific kinetic energy of the reference radiation field as well as the absorbed dose of pyroe-

lectric light to verify the uniformity of the radiation field and the scattering contribution, respectively.

### 3.1. Model Building

The Monte Carlo software is used to model the dimensions and materials designed in “Heading 2”, and simulate the properties of scattering and uniformity in the irradiation field of the reference radiation field with reference to GB/T 12162.1-2000, and analyze the results to optimize the design. The design model is shown in **Figure 4**, where b is the unattenuated model and c is the attenuated model.

**Table 1.** Air specific kinetic energy ratio at each detection point.

Position of the detection point from the center of the ray beam (mm)	Relative Air Specific Kinetic Energy
0	100.00%
4.3	99.99%
8.6	99.96%
12.9	99.90%
17.2	99.82%
21.5	99.72%
25.8	99.60%
30.1	99.46%
34.4	99.30%
38.7	99.11%
43.0	98.91%
Inhomogeneity	1.09%

**Table 2.** Attenuator thickness at each reference point.

Radial Position (mm)	Attenuator Thickness (mm)
0	1.67
4.3	1.67
8.6	1.64
12.9	1.61
17.2	1.57
21.5	1.51
25.8	1.43
30.1	1.34
34.4	1.24
38.7	1.13
43.0	1.00

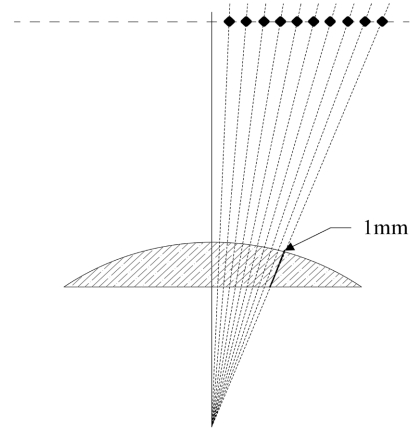


**Figure 3.** Schematic diagram of arc attenuator calculation.

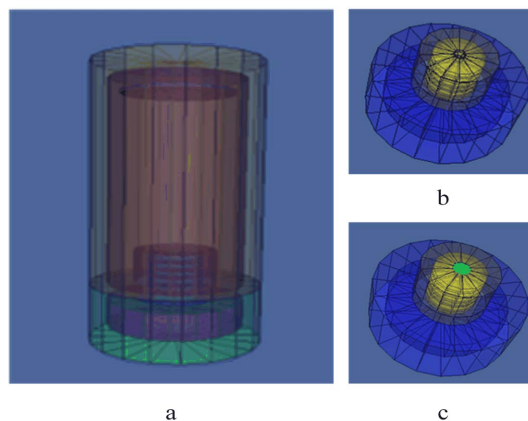


**Figure 4.** Monte Carlo model diagram of the irradiator.

### 3.2. Simulation of the Specific Kinetic Energy of Air

The air specific kinetic energy of the reference radiation field is simulated using Monte Carlo software. Since the whole model is a symmetrical structure, only one side of the irradiation field needs to be simulated and it extends beyond the irradiation field until it reaches the inner side of the shielded room. The simulation results are shown below.

#### 1) Inhomogeneity

The inhomogeneity of the reference radiation field is 1.18% obtained from the calculation results, which meets the relevant requirements. The dose values of each reference point of the radiation field without attenuator are shown in **Table 3**. The homogeneity simulation results are shown in **Figure 5**.

#### 2) Scattering

Radiation field scattering is modeled in two ways. One, the scattering is analyzed within the irradiation field. Second, the scattering was analyzed outside the irradiation field. The results are shown in **Table 4**.

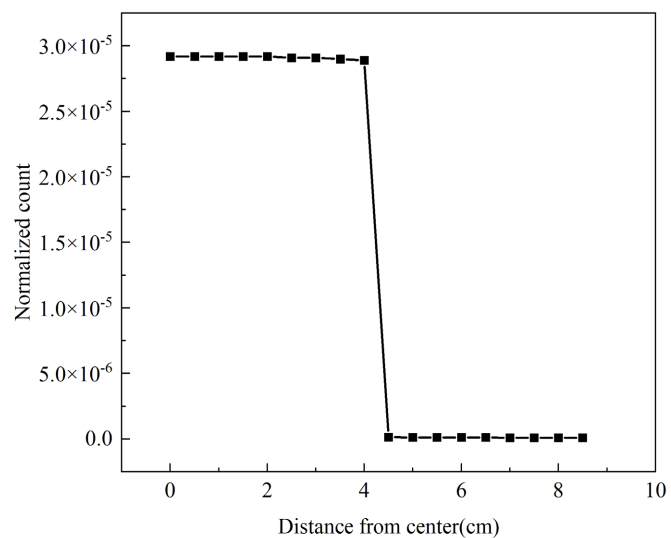
It can be concluded from the results that the scattering contribution is less than 5% both in the irradiation and in the field, which meets the design requirements.

**Table 3.** Dose values at reference points of the radiation field without attenuator.

Reference Point within the Irradiation Field		Reference Point outside the Irradiated Field	
Distance from Center (cm)	Normalized Count	Distance from Center (cm)	Normalized Count
0.0	2.92E-05	4.5	1.37E-07
0.5	2.92E-05	5.0	1.14E-07
1.0	2.92E-05	5.5	1.09E-07
1.5	2.92E-05	6.0	1.08E-07
2.0	2.92E-05	6.5	1.06E-07
2.5	2.91E-05	7.0	1.05E-07
3.0	2.91E-05	7.5	1.04E-07
3.5	2.90E-05	8.0	1.03E-07
4.0	2.89E-05	8.5	1.02E-07

**Table 4.** Air specific kinetic energy scattering contribution.

Reference Point within the Irradiation Field		Reference Point outside the Irradiated Field	
Distance from Center (cm)	Scattering Contribution	Distance from Center (cm)	Scattering Contribution
0.0	3.56%	4.5	2.49%
0.5	3.55%	5.0	2.22%
1.0	3.52%	5.5	1.80%
1.5	3.46%	6.0	1.43%
2.0	3.38%	6.5	1.16%
2.5	3.28%	7.0	0.98%
3.0	3.17%	7.5	0.84%
3.5	3.06%	8.0	0.74%
4.0	2.95%	8.5	0.67%

**Figure 5.** Homogeneity simulation results.

### 3.3. Simulation of Absorbed Dose in TLD

For the simulation of the absorbed dose of the TLD, the thermoluminescent grating element is arranged on one side in the thermoluminescent pallet and extends beyond the irradiation field until it reaches the edge of the thermoluminescent pallet.

#### 1) Inhomogeneity

The simulation results are shown in **Figure 6**.

The results of the calculations show that the inhomogeneity of the radiation field within the irradiation field reaches 1.81%. It meets the requirements of the relevant standards.

#### 2) Scattering

The dose values detected by the TLD in the irradiated field were all contributed by scattered rays, and the contribution of scattered rays was 0.97% of the average value of the dose values in the irradiated field. The requirements of the relevant standards have been met.

### 3.4. Simulation of Arc Attenuator Correction

The following section focuses on describing the corrections to the specific kinetic energy of the air in the radiation field with the addition of an attenuator.

#### 1) Inhomogeneity

The results of the dose value of each reference point of the radiation field after adding the attenuator are shown in **Table 5**, and the inhomogeneity of the reference radiation field after adding the attenuator is calculated to be 0.26%, which meets the relevant requirements. The inhomogeneity of the radiation field without the attenuator is 1.18%, and after the attenuator is added, the inhomogeneity is corrected to 0.26%, and the attenuator has a good effect in improving the uniformity of the radiation field.

#### 2) Scattering

The changes in radiation field scattering in the irradiated field after the addition of the attenuator are shown in **Table 6**.

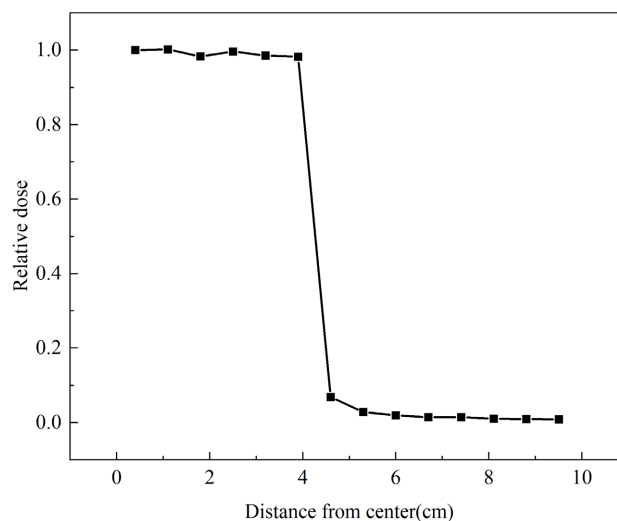


**Figure 6.** Absorbed dose simulation results.



**Table 5.** Dose values at reference points of the radiation field after attenuator addition.

Reference Point within the Irradiation Field		Reference Point outside the Irradiated Field	
Distance from Center (cm)	Normalized Count	Distance from Center (cm)	Normalized Count
0.0	2.85E-05	4.5	1.40E-07
0.5	2.85E-05	5.0	1.16E-07
1.0	2.85E-05	5.5	1.12E-07
1.5	2.85E-05	6.0	1.10E-07
2.0	2.85E-05	6.5	1.08E-07
2.5	2.85E-05	7.0	1.07E-07
3.0	2.85E-05	7.5	1.05E-07
3.5	2.84E-05	8.0	1.03E-07
4.0	2.84E-05	8.5	1.01E-07

**Table 6.** Comparison of kinetic energy scattering contribution from air ratio release.

No Attenuator		With Attenuator	
Distance from Center (cm)	Scattering Contribution	Distance from Center (cm)	Scattering Contribution
0.0	3.56%	0.0	3.54%
0.5	3.55%	0.5	3.54%
1.0	3.52%	1.0	3.50%
1.5	3.46%	1.5	3.46%
2.0	3.38%	2.0	3.37%
2.5	3.28%	2.5	3.28%
3.0	3.17%	3.0	3.17%
3.5	3.06%	3.5	3.06%
4.0	2.95%	4.0	2.96%

It can be obtained from the results that the low-energy scattering of the radiated field is partially shielded after the addition of the attenuator. But the shielding share is small.

#### 4. Conclusion

The results show that the shielding performance, radiation field uniformity, scattering contribution rate and other indexes of the simple standard irradiator meet the requirements of the standards, and can calibrate more than 50 thermoluminescent detectors at one time. The designed simple standard irradiator can meet the calibration and scale requirements of pyroelectric detectors for environmental dose monitoring.

#### Acknowledgements

The authors gratefully acknowledge the financial support from the Sichuan

---

Province Ecological Environmental Protection Science and Technology Program (NO. 2021HB11).

### Conflicts of Interest

The authors declare no conflicts of interest.

### References

- [1] Nika, G., Michael, F., Saravanabavaan, S., *et al.* (2017) Radiation Dose Monitoring in the Clinical Routine. *Fortschritte auf dem Gebiete der Rontgenstrahlen und der Nuklearmedizin*, **4**, 356-360. <https://doi.org/10.1055/s-0042-116684>
- [2] Wang, X., Cheng, Y., Qi, M.S., *et al.* (2013) Study on Dose Performance of LiF (Mg, Cu, P) Thermoluminescence Detectors. *Atomic Energy Science and Technology*, **47**, 1888-1891.
- [3] Knežević, M.M., Baranowska, Z., *et al.* (2021) Investigations into the Basic Properties of Different Passive Dosimetry Systems Used in Environmental Radiation Monitoring in the Aftermath of a Nuclear or Radiological Event. *Radiation Measurements*, **146**, 106615. <https://doi.org/10.1016/j.radmeas.2021.106615>
- [4] (2000) PRC State Bureau of Quality and Technical Supervision. X and Gamma Reference Radiation for Calibrating Dosemeters and Doserate Meters and for Determining Their Response as a Function of Photon Energy: Part 1: Radiation Characteristics and Production Methods. GB/T 12162. 1-2000. Standard Press of China, Beijing.
- [5] (2019) Standardization Administration of China. Specification for Design Construction and Use of Gamma Irradiation Facilities. GB/T 17568-2019. Standard Press of China, Beijing.
- [6] Xia, Y.H. (2010) Course on Advanced Ionizing Radiation Protection. 5th Edition. Harbin Engineering University Press, Harbin.
- [7] (2016) PRC State Administration of Quarantine. Thermoluminescence Dosimetry Systems Used in Personal and Environmental Monitoring for X- and  $\gamma$ -Radiation. JJG 593-2016. China Quality Inspection Press, Beijing.